

Sliding Window-Aided Ordered Statistics Decoding for Short LDPC Codes

Guangwen Li, Xiao Yu

Abstract—This paper introduces an innovative approach to the design of efficient decoders that meet the rigorous requirements of modern communication systems, particularly in terms of ultra-reliability and low-latency. We enhance an established hybrid decoding framework by proposing an ordered statistical decoding scheme augmented with a sliding window technique. This novel component replaces a key element of the current architecture, significantly reducing average complexity. A critical aspect of our scheme is the integration of a pre-trained neural network model that dynamically determines the progression or halt of the sliding window process. Furthermore, we present a user-defined soft margin mechanism that adeptly balances the trade-off between decoding accuracy and complexity. Empirical results, supported by a thorough complexity analysis, demonstrate that the proposed scheme holds a competitive advantage over existing state-of-the-art decoders, notably in addressing the decoding errors prevalent in neural min-sum decoders. Additionally, our research uncovers that short LDPC codes can deliver performance comparable to that of short classical linear codes within the critical waterfall region of the SNR, highlighting their potential for practical applications.

Index Terms—Deep learning, Neural network, Belief propagation, Min-Sum, Training

I. INTRODUCTION

Channel coding is essential for robust information transmission in telecommunication systems. Gallager’s low-density parity-check (LDPC) codes, in particular, have distinguished themselves for their superior error correction capabilities, approaching the theoretical Shannon limit asymptotically [1], [2]. In contexts such as the Internet of Things (IoT), where low complexity and minimal latency are crucial, computational limitations often necessitate the use of approximations like min-sum (MS) variants over standard belief propagation (BP) decoders [3], [4].

However, for practical finite-length LDPC codes, simplified MS versions widen the performance gap from maximum likelihood (ML) decoding. Nachmani et al. [5] pioneered an approach that integrates BP iterations into a neural network (NN) with trainable parameters for each edge, addressing the ‘curse of dimensionality’ in code space. This method has been adapted to mitigate the complexity associated with standard BP functions, with NN adaptations for normalized min-sum (NMS) and offset min-sum (OMS) decoders demonstrating remarkable performance for certain classical block codes [6]–[10]. Buchberger et al. [11] proposed a neural BP with decimation (NBP-D) scheme that integrates an NN to determine vari-

able node decimation, effectively ensembles multiple decoding results, albeit with substantial computational complexity.

Concurrently, ordered statistical decoding (OSD) and its variants have been explored to reduce complexity while sustaining performance across various codes. Criticisms of the original OSD [12] center on its escalating computational complexity with increasing order- p , or the Hamming weight of its test error patterns (TEPs). Recent variants [13]–[15] offer alternatives for approaching ML decoding of extended BCH (eBCH) codes or RS codes, known for their large minimum distance, potentially meeting the stringent requirements of 6G or IoT standards [16]. These strategies commonly employ threshold techniques to bypass certain TEPs or terminate decoding early based on the evaluation of current TEPs. For instance, a probability-based scheme in [13] derives two adaptive thresholds for received sequences, guiding the sequential checking of TEPs generated with a tree-like structure. In [14], lifted lower bounds facilitate early termination checks before each re-encoding phase within order- p OSD, alongside other thresholds for updating the optimal estimate or exiting OSD. Strategies incorporating reliability information from bits in the least reliable basis (LRB) adjacent to the most reliable basis (MRB) have also been explored to impose additional constraints on decoding and reduce the OSD search space [17]–[20]. In summary, most state-of-the-art (SOTA) OSD variants for classical linear codes focus on strategically selecting and scheduling a minimal number of TEPs for each received sequence to maximize decoding performance, yet they often suffer from high latency due to serial processing of TEPs.

In the domain of short LDPC codes, addressing decoding errors in BP due to dominant absorbing sets, a combination of recurrent neural network (RNN) models trained for each dominant absorbing set and OSD has claimed near-ML decoding performance [21]. However, the extensive training and complex implementation have limited its adoption. To overcome these challenges, we introduced the NMS-DIA-OSD framework for LDPC codes in prior research [22], which achieves a favorable balance between performance, complexity, and throughput. Specifically, to tackle NMS decoding errors, iterative trajectories are synthesized via a neural model to produce a new reliability metric, decoding information aggregation (DIA). This DIA has been shown to significantly benefit the subsequent adaptive OSD, which incorporates the historical distribution of error patterns into the current decoding task.

Building on the case-by-case strategy of OSD variants, we propose a new sliding window-aided OSD as an extension of

arXiv:2404.14165v2 [cs.IT] 28 Apr 2024

G.Li is with the College of Information & Electronics, Shandong Technology and Business University, Yantai, China e-mail: lgwa@sdu.edu.cn

X.Yu is with the Department of Physical Sports, Binzhou Medical University, Yantai, China e-mail: YuXiao@bzmc.edu.cn

our previous work, substituting for the adaptive OSD component in the NMS-DIA-OSD framework. This mechanism leverages a two-layered neural model, with softmax outputs providing soft information for the decision to terminate the current OSD early or continue. Retaining the low latency characteristic of the NMS-DIA-OSD framework, the new framework further reduces computational complexity and demonstrates competitive performance against SOTA decoders for short LDPC codes, offering a better trade-off when handling NMS decoding errors. Additionally, it is observed that short LDPC codes and short eBCH codes of the same rate and length exhibit near-competitive efficacy in decoding performance and computational complexity.

The remainder of this paper is organized as follows: Section II outlines essential preliminaries on BP decoding variants, DIA, and OSD variants. Section III details the motivations and our proposed sliding window-aided OSD. Section IV presents experimental results and complexity analysis. Finally, Section V concludes the paper with remarks and suggestions for further research.

II. PRELIMINARIES

Consider a binary message vector $\mathbf{m} = [m_i]_1^K$. The encoder converts this message into a codeword $\mathbf{c} = [c_i]_1^N$ through matrix multiplication $\mathbf{c} = \mathbf{m}\mathbf{G}$ over the Galois Field $\text{GF}(2)$, where K and N denote the lengths of the message and codeword, respectively. For simplicity, the generator matrix \mathbf{G} is assumed to be full-rank.

Following the encoding process, binary phase shift keying (BPSK) modulation is applied, which maps each codeword bit c_i to a symbol $s_i = 1 - 2c_i$. The received sequence $\mathbf{y} = [y_i]_1^N$ is then observed at the channel output, with $y_i = s_i + n_i$ representing the received symbol corrupted by additive white Gaussian noise n_i with zero mean and variance σ^2 .

Assuming symbols are sent with equal probability, the log-likelihood ratio (LLR) for the i -th bit is derived as:

$$l_i = \log \left(\frac{p(y_i | c_i = 0)}{p(y_i | c_i = 1)} \right) = \frac{2y_i}{\sigma^2}. \quad (1)$$

Traditionally, the magnitude of y_i is a reliable indicator for gauging the confidence in the hard decision \hat{c}_i for the i -th bit, where $\hat{c}_i = \mathbf{1}(y_i < 0)$ and $\mathbf{1}(\cdot)$ is the indicator function.

A. NMS and its Neural Version

Traditional NMS decoding aims to replace the complex \tanh or \tanh^{-1} functions of BP with weighted approximations during check node updates. Treating the NMS decoder as a simple neural network within the NBP family allows it to obtain a single weight. Consequently, a well-trained NMS can significantly narrow the performance gap between the MS and BP.

However, for short LDPC codes, the inherent error floor effect prevents NMS or NBP from approaching their ML performance. To address this, one common approach is to employ OSD as a post-processing step for failed NMS decoding cases [23].

B. DIA and OSD Variants

1) *Conventional OSD*: OSD variants are considered universal decoders [12] as they do not depend on any specific channel noise characteristics. Some variants focus on GE operations with respect to the generator matrix \mathbf{G} , while others involve transformations of the parity check matrix \mathbf{H} . Typically, there is no significant difference in performance between these two types of variants due to the highly symmetrical steps in their respective OSD implementations. The two benchmark decoders mentioned in Section IV are implemented as originally described [13], [14]. Our proposed scheme will concentrate on the latter approach due to its slightly lower complexity requirement when performing GE to reduce the sparse \mathbf{H} of LDPC codes.

Algorithm 1 Conventional order- p OSD

Input: Received sequence $\mathbf{y} = [y_i]_1^N$, parity check matrix \mathbf{H}

Output: Optimal codeword estimate $\hat{\mathbf{c}}$

- 1: Sort $[y_i]_1^N$ in ascending order of magnitude to obtain $\mathbf{y}^{(1)} = [y_i^{(1)}]_1^N$. Correspondingly, transform \mathbf{H} into $\mathbf{H}^{(1)}$ via column permutation.
 - 2: Reduce $\mathbf{H}^{(1)}$ to its systematic form $\mathbf{H}^{(2)} = [\mathbf{I} : \mathbf{Q}_2]$. This step identifies all bit positions as either in the LRB or the MRB blocks, leading to the rearrangement of $\mathbf{y}^{(1)}$ into $\mathbf{y}^{(2)} = [y_i^{(2)}]_1^N$.
 - 3: Obtain a hard decision \mathbf{c}_a from $[y_i^{(2)}]_{N-K+1}^N$ as an anchor point.
 - 4: **for** $i \in \{0, 1, 2, \dots, p\}$ **do**
 - 5: **repeat:** (Phase- i re-encoding of OSD)
 - 6: Generate the codeword candidates $\bar{\mathbf{c}}_j = [\bar{c}_{1j} : \bar{c}_{2j}]$ for each TEP \mathbf{e}_j of Hamming weight i , where $\mathbf{e}_j \oplus \mathbf{c}_a \Rightarrow \bar{\mathbf{c}}_{2j}$, $\bar{c}_{1j} = \bar{c}_{2j} \mathbf{Q}_2^\top$ due to parity check constraints.
 - 7: Add the candidate $\bar{\mathbf{c}}_j$ to the list of codeword candidates.
 - 8: **until** traversing is complete
 - 9: **end for**
 - 10: Select the optimal $\tilde{\mathbf{c}}$ from the list of codeword candidates based on criterion 2, then reverse all involved bit swaps to obtain $\hat{\mathbf{c}}$.
 - 11: **return** the optimal codeword estimate $\hat{\mathbf{c}}$ for \mathbf{y} .
-

For conventional order- p OSD, the allowed Hamming weight of all its TEPs is at most p . Essentially, it involves searching for the optimal solution within a manageable complexity. The pseudo-code for the \mathbf{H} -oriented order- p OSD is depicted in Algorithm 1. Specifically, after sorting the received sequence based on the reliability metric in step 1 and performing GE operations on \mathbf{H} in step 2, the leftmost bits form the LRB and the remaining bit positions form the MRB, as indicated by $\mathbf{H}^{(2)} = [\mathbf{I} : \mathbf{Q}_2]$. Subsequently, all codeword candidates $\bar{\mathbf{c}}_j$, $j \in \{1, 2, \dots, \sum_{i=0}^p \binom{K}{i}\}$ derived in step 6, are evaluated for optimality using the criterion [12]:

$$\tilde{\mathbf{c}} = \arg \min_{\bar{\mathbf{c}}_j = [c_i]_1^N} \sum_{i=1}^N \mathbf{1}(\tilde{c}_i \neq c_i) \left| y_i^{(2)} \right| \quad (2)$$

where \tilde{c}_i is the hard decision of $y_i^{(2)}$ (the i -th entry of $\mathbf{y}^{(2)}$).

Ultimately, the appropriate bit swaps of \tilde{c} are reversed to yield the optimal estimate \hat{c} for y .

2) *DIA and Adaptive OSD*: In our prior work [22], we introduced DIA to serve as a substitute for the magnitude of the received sequence in terms of reliability metrics. Specifically, DIA is implemented as a four-layered neural network model that processes the bit trajectory associated with each failed NMS iterative decoding attempt. The output of this model has been statistically validated to enhance reliability measurements, thereby maximizing the effectiveness of OSD of a given order- p for NMS decoding errors in short LDPC codes.

Although the conventional OSD can asymptotically approach ML performance for $p \geq \lceil \frac{d_{min}}{4} - 1 \rceil$, where d_{min} represents the minimum distance of the code [12], its utility is significantly hindered by the polynomial growth of complexity $O(N^p)$ with respect to the order- p . An adaptive OSD, supported by DIA, addresses this challenge by offering competitive decoding performance while minimizing complexity. Additionally, it retains the parallel decoding mode of conventional OSD to ensure low latency.

Unlike conventional OSD, the adaptive OSD includes an additional query phase to gather the statistical distribution of actual error patterns associated with existing NMS decoding errors. First, all TEPs with a given order- p are categorized into blocks known as order patterns. Then these order patterns are prioritized based on the ratio of the number of included genuine error patterns to the size of each order pattern. During the OSD decoding phase, the TEPs along the decoding path, which is a sequence of order patterns, are examined when selecting codeword candidates for the optimal estimate of the transmitted codeword. Consequently, steps 4-9 of Algorithm 1 are adapted accordingly. For a more detailed explanation of DIA and adaptive OSD, interested readers are directed to [22].

III. SLIDING WINDOW-AIDED OSD

A. Flow Chart of NMS-DIA-OSD

Drawing inspiration from the case-by-case strategy characteristic of existing SOTA OSD decoders as detailed in Section I, we have integrated a novel sliding window-aided OSD noted as OSD_{SW} to supplant the adaptive OSD component within the NMS-DIA-OSD framework, leaving all other elements intact. This modification is graphically represented in Fig. 1. The newly introduced OSD variant, functioning as a partially parallel derivative of the adaptive OSD, is designed to markedly decrease the average computational complexity—quantified by the number of TEPs—with only a nominal impact on decoding performance.

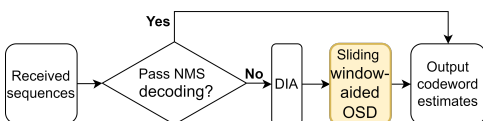


Fig. 1. Block flow chart illustrating the NMS-DIA-OSD decoding process.

B. Sliding Window Model

1) *Observations*: Consider the LDPC CCSDS (128,64) code [10], where partitioning the MRB yields $Q = 6$ segments delineated by the bit indices $[0, 5, 15, 22, 28, 40, 64]$. Assuming an actual decoding path length $\hat{l}_{pt} = 12$, then the first 12 order patterns that persist post-truncation are selected for analysis. The minimum distances to each order pattern from the received sequence are computed based on the minimum weighted Hamming weight evaluation between the corresponding TEPs of each order pattern and the received sequence, as depicted by (2). With ample sampling, the indices of the order patterns corresponding to genuine error patterns serve as labels for supervised machine learning, resulting in $\hat{l}_{pt} + 1 = 13$ distinct classes, with failure cases categorized under an additional class labeled '-1'.

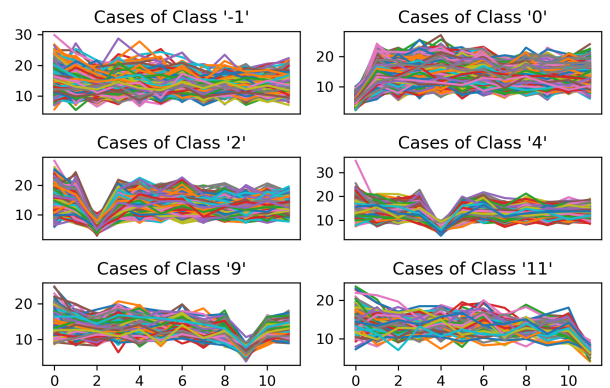


Fig. 2. Piece-wise plots of classified minimum distance lists for the LDPC CCSDS (128,64) code at SNR=2.7dB. The statistical spikes in each subplot correspond to the minimum distances for genuine error patterns, while cases labeled '-1' represent exceptions to the specified decoding path length $\hat{l}_{th} = 12$.

From Fig. 2, we can deduce the following: Firstly, aside from the '-1' class representing failure cases, which lack pronounced spikes, classes corresponding to specific order patterns exhibit distinct spikes in their minimum distance lists. This justifies the incorporation of an early termination feature in our proposed OSD_{SW} . Secondly, an increased window width W_d correlates with a decreased risk in the decision to terminate early; setting $W_d = \hat{l}_{th}$ eliminates the need for sliding, resulting in the adaptive OSD from [22], which, while having the highest complexity due to its exhaustive traversal of TEPs, does not compromise performance. The selection of W_d is thus critical in balancing decoding performance with complexity. Lastly, while the spike characteristic is apparent in global minimum distance lists, challenges arise when examining a local sliding window with a unit stride. The optimal decision, ideally made after observing all associated order patterns, must be weighed against the need for an immediate decision to either slide the window or exit. A simple thresholding approach is initially appealing but is insufficient for handling complex noise patterns and lacks adaptability, which can result in performance degradation. To navigate this trade-off while minimizing performance loss and maximizing complexity reduction, we propose leveraging a neural model.

To enhance the accuracy rate, the multi-label classification challenge is streamlined into a binary-label problem: Given the elements within the current window, the decision is whether to proceed with sliding the window or to exit immediately.

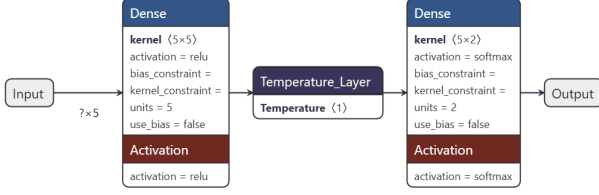


Fig. 3. The fully connected neural network architecture of the sliding window model for early termination estimation with a window width of $W_d = 5$.

2) *Model Architecture*: As depicted in Fig. 3, our approach to determining the optimal moment for early termination decoding involves a neural network composed of two 'Dense' layers from the Keras package [24]. These layers are interleaved with a custom temperature layer that scales the input using a single trainable parameter. The activation functions for the 'Dense' layers are 'relu' and 'softmax', respectively, indicating that the model's output is a binary decision's probability distribution. The neural network is designed with W_d neurons in the first layer and 2 neurons in the second layer, tailored for this specific code. It is worth noting that the model's configuration can be fine-tuned experimentally for optimal performance.

3) *Training Logistics*: For each NMS decoding error, the DIA output generates a distinct minimum distance list for each order pattern within the given decoding path of length \hat{l}_{th} . A sequence of sliding windows of width W_d with a unit stride are recorded, forming the training samples. These samples are labeled '1' if the global minimum element of the minimum distance list falls within the current window, or '0' to signal the continuation of window sliding. After compiling and shuffling a sufficient number of samples, the training dataset is constructed. To counteract class imbalance, we employ APIs in Tensorflow to assign varying weights to individual samples during training.

Optimizing the model parameters is performed using stochastic gradient descent (SGD) methods, such as the Adam optimizer [25], with a regularized cross-entropy loss function defined as follows:

$$\ell_{ce} = \sum_{i=1}^{b_n} \left(\sum_{j=0}^1 p(d_i = j) \cdot \log \frac{1}{p(\hat{d}_i = j)} + \alpha \cdot L_i^s \right) \quad (3)$$

with

$$L_i^s = \mathbf{1}(p(\hat{d}_i = 1) > p(\hat{d}_i = 0) | p(d_i = 0) = 1)$$

where b_n is the batch size, $p(d_i = j)$ is the ground truth probability for the binary value of the i -th sample, $p(\hat{d}_i = j)$ is the estimated probability from the softmax output of the sliding window model, L_i^s is a regularization term penalizing premature termination, and $\alpha = 10.0$ serves as the regularization coefficient.

An initial learning rate of 0.001 is selected to address divergence due to oscillation or slow convergence, with a

decay rate of 0.95 every 500 training steps. Training typically stabilizes within 5000 steps, which can be completed within a few minutes on a personal computer with a '2.60GHz Intel i7-6700HQ' processor.

C. Proposed OSD algorithm

The pseudo-code for the OSD_{SW} is presented in Alg. 2, with modifications from the conventional order- p OSD (Alg. 1) highlighted in blue.

In step 4, the minimum distances for the window width W_d are identified through an exhaustive search, akin to steps 6-7 of Alg. 1. Step 5 emphasizes that a new minimum distance within the window triggers the sliding window model only if it is less than the current global minimum. To minimize performance degradation, a soft margin $s_m > 0$ is introduced in step 0 of Alg. 2 to manage the trade-off between performance and complexity. The sliding window model's decision for early termination is made with a high degree of confidence, akin to hypothesis testing. Notably, when s_m increases to one, the performance of OSD_{SW} mirrors that of the adaptive OSD, processing all TEPs without early termination. Lastly, finding W_d minimum distances in step 4 can be efficiently performed using vector computing, making sliding window OSD a partially parallel implementation of OSD.

Algorithm 2 Sliding window-aided OSD

Input: Received sequence $\mathbf{y} = [y_i]_1^N$, \mathbf{H} , reliability metric $\tilde{\mathbf{y}} = [\tilde{y}_i]_1^N$ from DIA output, predetermined actual decoding path of length \hat{l}_{pt} , window width W_d , soft margin s_m .

Output: Optimal codeword estimate $\hat{\mathbf{c}}$

- 1: Repeat operations from step 1-3 of Alg. 1, substituting $[\tilde{y}_i]_1^N$ for $[y_i]_1^N$.
 - 2: Initialize the current minimum weighted distance d_w to ∞ , and align the initial window with the first W_d order patterns.
 - 3: **repeat:**
 - 4: Generate the W_d minimum distances from the current window's order patterns. Record the minimum element $d_{w,c}$.
 - 5: **if** $d_{w,c} < d_w$ **then**
 - 6: Input the sorted W_d elements into the sliding window model to obtain binary decision probabilities $[P_0, P_1]$. Update $d_w = d_{w,c}$.
 - 7: **if** $P_1 - P_0 > s_m$ **then**
 - 8: Break Early Termination
 - 9: **end if**
 - 10: **end if**
 - 11: Slide the window along the decoding path with a unit stride.
 - 12: **until** Reaching the end of the decoding path.
 - 13: Select the optimal $\hat{\mathbf{c}}$ based on the d_w evaluation and reverse all involved bit swaps for $\hat{\mathbf{c}}$ to obtain $\hat{\mathbf{c}}$.
 - 14: **return** the codeword estimate $\hat{\mathbf{c}}$ for \mathbf{y} .
-

IV. EXPERIMENTAL RESULTS AND COMPLEXITY ANALYSIS

All schemes were implemented in Python and simulations were conducted using the TensorFlow platform. To ensure the stability of the results, we collected at least 100 decoding errors at each specific SNR before concluding the tests.

A. Parameter Settings of Codes

For the LDPC CCSDS (128,64) code [10] within the NMS-DIA-OSD_{SW} framework, we set the maximum number of iterations to $T = 12$ and the normalization parameter to $\alpha = 0.78$, trained at SNR=2.7dB for the NMS component. The DIA model is presumed to be well-trained, and the OSD_{SW} decoding path is predetermined with $Q = 6$ segments when partitioning the MRB. The D-O($\lambda_m, \hat{l}_{th}, s_m$), which denotes the combination of DIA and OSD_{SW} with $W_d = 5$, is referenced in the subsequent plots. Here, λ_m represents the Hamming weight sum threshold for order patterns [22], analogous to the order- p in the original OSD. As benchmarks, PB-OSD [13] and FS-OSD [14], both with order- $p = 3$, are SOTA decoders that balance the number of TEPs required against decoding performance for eBCH codes. For PB-OSD, two evaluations are adapted for the two thresholds to assess their effectiveness on LDPC codes, noted as PB_{0,2} [22]. For FS-OSD, referred to as FS in the legend, parameters are set as $\tau_E = 6$, $\beta = 0.1$, and $\tau_{PSC} = 30$ to match the performance of competing decoders.

The original PB-OSD of eBCH (128,64,22) code, as presented in [13], is calibrated to compare the complexity of our proposed hybrid framework for the LDPC (128,64,14) code in terms of the average number of TEPs N_{at} and floating-point operations (FLOPs).

B. Decoding Performance

We begin by assessing the performance of the PB and FS variants for LDPC codes after necessary adaptation. As noted in [23], the NMS scheme is favored for its simplicity, high throughput, and independence from channel noise variance. Thus, we compare the PB and FS variants as post-processors for NMS decoding errors against the proposed OSD_{SW}.

Figures 4 and 5 present the decoding performance in terms of Frame Error Rate (FER) and complexity in terms of N_{at} , respectively. PB₀, which adheres to the original threshold evaluation from [13], exhibits the poorest FER performance. After re-evaluation, PB₂ shows significant improvement with a slight increase in complexity. FS-OSD offers marginally better performance than PB₂ but at a considerably higher complexity. In contrast, D-O(3,30,1.0), equivalent to the adaptive OSD with $\lambda_m = 3$ and $\hat{l}_{th} = 30$, is less attractive considering its performance and complexity. However, by extending \hat{l}_{th} to 40 and 50 and reducing s_m to 0.9, our sliding window technique effectively manages complexity while outperforming PB₂ in most SNR regions of interest.

In Fig. 6, the final FER of our hybrid framework, a product of NMS' FER and OSD_{SW}'s FER, is compared with the existing NBP variants. The NBP-D(10,4,4) [11], which incorporates a learned decimation step, significantly outperforms

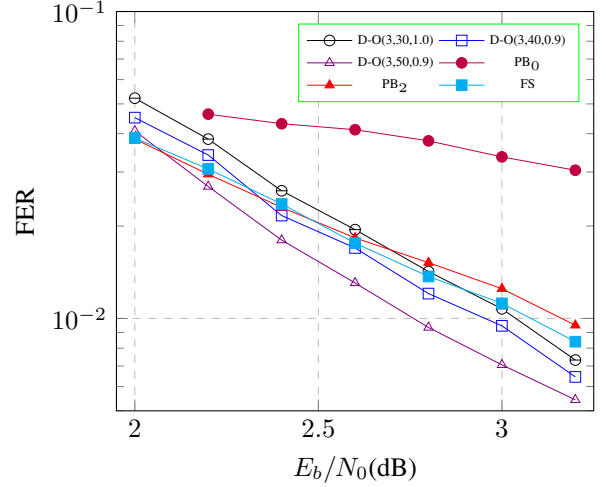


Fig. 4. FER comparisons for varied decoding schemes of LDPC (128,64) code in post-processing of NMS decoding failures.

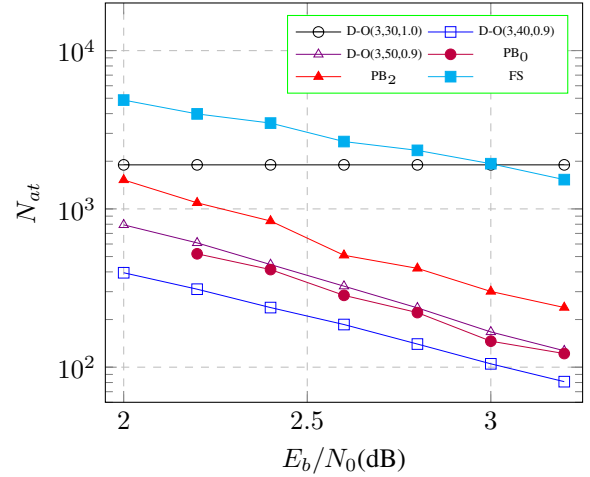


Fig. 5. Average number of TEPs N_{at} requested for LDPC (128,64) code under different schemes.

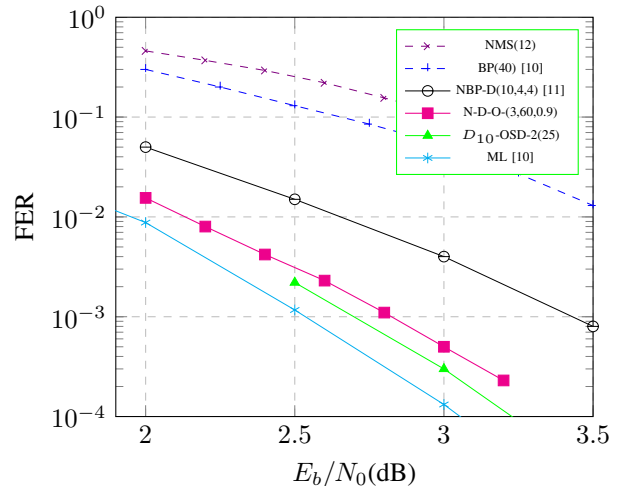


Fig. 6. FER comparison for various decoding schemes of LDPC (128,64) code

NMS or BP but falls behind N-D-O(3,60,0.9) by at least 0.5dB at FER= 10^{-3} . N-D-O(3,60,0.9) is slightly behind the SOTA D₁₀-O-0(25) [21] by about 0.1dB, although its complexity is considerably lower. Both schemes are within 0.3dB of the ML performance, as depicted in Fig. 6.

C. Complexity Analysis

For the LDPC (128,64) code, with average row and column weights of $(w_c, w_r) = (4, 8)$, the average number of iterations for NMS is denoted as I_{at} and the average number of windows shifted for the sliding window technique as W_{at} . The average complexity C_{av} per received sequence for the hybrid decoding framework can be approximated by:

$$C_{av} = C_{NMS} + \tau(C_{OSD} + C_{DIA} + C_{SW})$$

Here, τ represents the FER of NMS when undetectable decoding errors are negligible, and C_{DIA} , C_{SW} denote the complexities of the DIA model and sliding window model respectively.

As detailed in Table I, with increasing SNR, W_{at} decreases from 7.6 to 2.3, indicating greater confidence in early termination following the initial order pattern tests. Benchmarked by the high-complexity implementation of conventional OSD, its SOTA OSD variants and the proposed framework are compared for the eBCH code and short LDPC codes of the same length and rate respectively. Conditioned on a rival FER from SNR=2.0dB to SNR=3.0dB, in terms of complexity measured by the average count of TEPs N_{at} and FLOPs, it reveals that the original PB-OSD is approximately half to a quarter of the proposed framework. Despite this, the straightforward implementation of arithmetic operations and independence from channel noise variance make the latter an attractive alternative. Furthermore, in latency-sensitive scenarios, OSD_{SW} is preferable due to its partial parallelization, allowing rapid post-processing of TEPs in batch mode, as verified by simulations that show OSD_{SW} to be at least two orders of magnitude faster than the PB-OSD or FS-OSD in collecting 100 failure cases when post-processing NMS decoding errors. For the worst-case complexity of decoding, our proposed N-D-O_{SW}(3, 60, 0.9) requires a constant number of TEPs (43,745 and 12,447 respectively), while PB-OSD's demand varies around 10,000 for specific SNR points.

TABLE I
COMPLEXITY COMPARISON OF VARIOUS DECODING SCHEMES FOR LDPC (128,64) AND EBCH (128,64) CODES

Codes Schemes	LDPC CCSDS (128,64) code		eBCH (128,64) code	
	N-D-O _{SW}	Original OSD	order-p = 3	PB-OSD [13]
Parameter Settings	$\lambda_m = 3$	order-p = 3	order-p = 3	order-p = 3
FER& I_{at} & W_{at} & N_{at} (SNR = 2.0dB)	1.55e-2 & 8.3 & 7.6 & 1344	1.4e-2 & 0 & 0 & 43745	1.6e-2 & 0 & 0 & 500	
FER& I_{at} & W_{at} & N_{at} (SNR = 2.5dB)	3.2e-3 & 6.4 & 4.1 & 609	3e-3 & 0 & 0 & 43745	3.3e-3 & 0 & 0 & 200	
FER& I_{at} & W_{at} & N_{at} (SNR = 3.0dB)	5e-4 & 4.6 & 2.3 & 249	5.4e-4 & 0 & 0 & 43745	5.6e-4 & 0 & 0 & 60	
C_{av} (FLOPs) (SNR = 2.0/2.5/3.0dB)	NMS		$32N_{at}^*$ $\approx 1.4/1.4/1.4M$	loosely lower bounded by $(\frac{2}{3} + 2)N_{at}$ $\approx 86.3/34.5/10.4K$
	DIA			
	OSD			
	SW	OSD		
	For $\tau = 0.447/0.24/0.10$.			
192/103/47K				

Note: * Half of the LRB length, equivalently 32 for the codes, is approximated for the count of FLOPs per re-encoding of weighted Hamming weight of (2).

V. CONCLUSIONS AND FUTURE RESEARCH

In this paper, we have introduced a novel sliding window adaptation of the OSD component within the NMS-DIA-OSD framework [22], which maintains the benefits of superior decoding performance, high throughput, and channel knowledge independence. This adaptation is particularly noteworthy for its ability to customize the decoding scheme for each received sequence, significantly reducing complexity. Specifically, the sliding window elements for a given sequence are processed through a lightweight neural model to determine whether to terminate or continue decoding early. The soft margin between the associated probabilities of this binary decision is easily adjustable, allowing for a convenient trade-off between performance and complexity. Our proposed scheme has been shown to outperform SOTA decoders designed for eBCH codes, particularly in the post-processing of NMS decoding errors for LDPC codes. Furthermore, a comparative analysis between LDPC and eBCH decoders of the same length and rate revealed that LDPC short codes are indeed competitive with eBCH codes, especially in the waterfall SNR region.

In the current setup, the DIA model accounts for the majority of the complexity at lower SNRs. To address this, simplifying the DIA model to a less complex neural network configuration could be explored without substantially affecting performance. Additionally, other hyperparameters, such as the window width W_d or the Q parameter in MRB partitioning, could be fine-tuned. Further research is needed to confirm whether these adjustments can effectively bridge the gap in computational complexity. Moreover, we conjecture that an advanced neural network, when trained on a sample subset from each order pattern of the decoding path, may accurately predict the ground truth order pattern. This would imply that only the TEPs corresponding to the final destination need to be evaluated to determine the optimal codeword estimate. While this approach presents significant challenges, it holds great promise and is a worthy direction for future investigation.

REFERENCES

- [1] Robert Gallager. Low-density parity-check codes. *IRE Trans. Inf. Theory*, 8(1):21–28, 1962.
- [2] David JC MacKay and Radford M Neal. Near shannon limit performance of low density parity check codes. *Electron. Lett.*, 32(18):1645, 1996.
- [3] Jianguang Zhao, Farhad Zarkeshvari, and Amir H Banihashemi. On implementation of min-sum algorithm and its modifications for decoding low-density parity-check (ldpc) codes. *IEEE Trans. Commun.*, 53(4):549–554, 2005.
- [4] Ming Jiang, Chunming Zhao, Li Zhang, and Enyang Xu. Adaptive offset min-sum algorithm for low-density parity check codes. *IEEE Commun. Lett.*, 10(6):483–485, 2006.
- [5] Eliya Nachmani, Yair Be'ery, and David Burshtein. Learning to decode linear codes using deep learning. In *2016 54th Annu. Conf. Commun., Control, and Comput. (Allerton)*, pages 341–346. IEEE, 2016.
- [6] Eliya Nachmani, Elad Marciano, Loren Lugosch, Warren J Gross, David Burshtein, and Yair Be'ery. Deep learning methods for improved decoding of linear codes. *IEEE J. Sel. Topics Signal Process.*, 12(1):119–131, 2018.
- [7] Fei Liang, Cong Shen, and Feng Wu. An iterative bp-cnn architecture for channel decoding. *IEEE J. Sel. Topics Signal Process.*, 12(1):144–159, 2018.
- [8] Loren Lugosch and Warren J Gross. Learning from the syndrome. In *2018 52nd Asilomar Conf. Signals, Syst., Comput.*, pages 594–598. IEEE, 2018.

-
- [9] Loren Peter Lugosch. *Learning algorithms for error correction*. McGill University (Canada), 2018.
- [10] Michael Helmling, Stefan Scholl, Florian Gensheimer, Tobias Dietz, Kira Kraft, Stefan Ruzika, and Norbert Wehn. Database of Channel Codes and ML Simulation Results. www.uni-kl.de/channel-codes, 2019.
- [11] Andreas Buchberger, Christian Häger, Henry D Pfister, Laurent Schmalen, and Alexandre Graell i Amat. Learned decimation for neural belief propagation decoders. In *2021-2021 Int. Conf. Acoust., Speech and Signal Process. (ICASSP)*, pages 8273–8277. IEEE, 2021.
- [12] Marc PC Fossorier and Shu Lin. Soft-decision decoding of linear block codes based on ordered statistics. *IEEE Trans. Inf. Theory*, 41(5):1379–1396, 1995.
- [13] Chentao Yue, Mahyar Shirvanimoghaddam, Giyoon Park, Ok-Sun Park, Branka Vucetic, and Yonghui Li. Probability-based ordered-statistics decoding for short block codes. *IEEE Commun. Lett.*, 25(6):1791–1795, 2021.
- [14] Changryoul Choi and Jechang Jeong. Fast and scalable soft decision decoding of linear block codes. *IEEE Commun. Lett.*, 23(10):1753–1756, 2019.
- [15] Baptiste Cavarec, Hasan Basri Celebi, Mats Bengtsson, and Mikael Skoglund. A learning-based approach to address complexity-reliability tradeoff in os decoders. In *2020 54th Asilomar Conf. Signals, Syst., and Comput.*, pages 689–692. IEEE, 2020.
- [16] Chentao Yue, Vera Miloslavskaya, Mahyar Shirvanimoghaddam, Branka Vucetic, and Yonghui Li. Efficient decoders for short block length codes in 6g urllc. *IEEE Commun. Mag.*, 61(4):84–90, 2023.
- [17] Lijia Yang, Wenhao Chen, and Li Chen. Reduced complexity ordered statistics decoding of linear block codes. In *2022 IEEE/CIC Int. Conf. Commun. in China (ICCC Workshops)*, pages 371–376. IEEE, 2022.
- [18] Jifan Liang, Yiwen Wang, Suihua Cai, and Xiao Ma. A low-complexity ordered statistic decoding of short block codes. *IEEE Commun. Lett.*, 27(2):400–403, 2022.
- [19] Chentao Yue, Mahyar Shirvanimoghaddam, Giyoon Park, Ok-Sun Park, Branka Vucetic, and Yonghui Li. Linear-equation ordered-statistics decoding. *IEEE Trans. Commun.*, 70(11):7105–7123, 2022.
- [20] Changryoul Choi and Jechang Jeong. Fast soft decision decoding of linear block codes using partial syndrome search. In *2020 IEEE Int. Symp. Inf. Theory (ISIT)*, pages 384–388. IEEE, 2020.
- [21] Joachim Rosseel, Valérian Mannoni, Inbar Fijalkow, and Valentin Savin. Decoding short ldpc codes via bp-rnn diversity and reliability-based post-processing. *IEEE Trans. Commun.*, 70(12):7830–7842, 2022.
- [22] Guangwen Li and Xiao Yu. Deep learning based enhancement of ordered statistics decoding of ldpc codes. *arXiv:2307.06575*, 2023.
- [23] Marco Baldi, Nicola Maturo, Enrico Paolini, and Franco Chiaraluce. On the use of ordered statistics decoders for low-density parity-check codes in space telecommand links. *EURASIP J. Wirel. Commun. Netw.*, 2016:1–15, 2016.
- [24] François Chollet et al. Keras. <https://keras.io>, 2015.
- [25] Diederik P Kingma and Jimmy Ba. Adam: A method for stochastic optimization. *arXiv:1412.6980*, 2014.